

Theory of Pseudogap Phenomena in High- T_c Cuprates Based on the Strong Coupling Superconductivity

Youichi YANASE* and Kosaku YAMADA

Department of Physics, Kyoto University, Kyoto 606-8502

(Received April 12, 1999)

In this paper we study the effects of the strong coupling superconductivity on the normal state electronic structure. We point out that the pseudogap phenomena in High- T_c cuprates are naturally explained as a precursor of the strong coupling superconductivity. We expand the reciprocal of the T-matrix with respect to the momentum and the frequency, and we discuss the properties of the expansion parameters. We estimate these parameters and carry out the calculations for the single particle self-energy using the T-matrix and the self-consistent T-matrix approximations, respectively. We show that the superconducting fluctuations, which are strongly diffusive within the conventional weak coupling theory, become propagative and have the character of the pre-formed pairs in the strong coupling case. The spectral weight and the density of states show the gap-like features by the effects of the resonances with the thermally excited weakly-damped pre-formed pairs. The spectral weight at the Fermi energy is strongly suppressed. This suppression starts at the mean field critical temperature T_{MF} and the actual critical temperature T_c is strongly reduced owing to the fluctuations. These features properly explain to the pseudogap phenomena in High- T_c cuprates.

KEYWORDS: high- T_c cuprates, pseudogap phenomena, strong coupling superconductivity, superconducting fluctuation, weakly damped pre-formed pair, resonance

§1. Introduction

Since the discovery of high-temperature (High- T_c) superconductivity by Bednortz and Müller,¹⁾ the anomalous normal state properties have been studied from the various points of view.

In particular, the pseudogap phenomena in under-doped cuprates have been a very important issue. There are a lot of studies for the issue from both experimental and theoretical points of view. However, the complete understanding remains to be obtained.

The pseudogap phenomena mean the suppression of the low frequency spectral weight without any long range order. They are universal phenomena observed in various compounds of under-doped cuprates.

* E-mail: yanase@ton.scphys.kyoto-u.ac.jp

The normal state excitation gap in under-doped cuprates have been indicated by several various experiments. The nuclear magnetic resonance (NMR) experiments have shown the anomalous temperature dependence of the spin lattice relaxation rate $1/T_1$ and the spin susceptibility χ .^{2,3)} The quantity $1/T_1T$, which increases with decreasing temperature, starts to decrease at the pseudogap onset temperature T^* .²⁾ The spin susceptibility decreases gradually from the rather high temperature, and immediately changes its slope at T^* .³⁾

The optical conductivity have indicated the suppression of the low frequency spectral weight above the superconducting critical temperature T_c .⁴⁾ The suppression is continuous above and below T_c .

The transport coefficients also change their behaviors at T^* . The T-linear in-plane resistivity observed in under-doped cuprates deviates downward.^{5,6)} The Hall coefficient remarkably deviates downward and decreases with temperature.⁵⁾ The c-axis resistivity strongly increases in the pseudogap region.⁷⁾ It have been shown that these behaviors of the transport phenomena are naturally explained by considering the momentum dependent scattering rate owing to the anti-ferromagnetic spin fluctuations.^{8,9)}

In particular, the angle-resolved photo-emission spectrum (ARPES)¹⁰⁾ experiments have directly shown the suppression of the low frequency spectral weight. Moreover, ARPES experiments have shown that the shape of the pseudogap is similar to that of the superconducting gap, and the magnitude does not change at the superconducting critical point.¹¹⁾ After all, the pseudogap has the d -wave shape and is continuously connected with the superconducting gap.

It is shown that the onset temperature T^* measured by the above experiments is almost the same as the mean field superconducting critical temperature T_{MF} estimated from the amplitude of the superconducting gap.⁶⁾

The recent tunneling experiments have directly shown the suppression of the low frequency density of states.¹²⁾ In this connection, the gap-like structure which is similar to the normal state pseudogap is observed in vortex cores in the superconducting states under the high magnetic fields.¹³⁾

The impurity effects on the reduction of T_c have indicated the suppression of the low frequency density of states.¹⁴⁾

The electronic specific heat is reduced well above T_c and T^* and the step height at T_c is extraordinary small in under-doped cuprates.¹⁵⁾ This means that the entropy has been already lost at rather high temperature.

From the above various experiments suggesting the relevance and continuity to the superconductivity, we consider that the pseudogap phenomena are the precursor of the strong coupling superconductivity. In this paper, we explain the pseudogap phenomena on the basis of the strong coupling superconductivity.

Several theoretical proposals have been given for the pseudogap phenomena. Here, we give a brief review on some important proposals.

One of them is the resonating valence bond (RVB) theory.¹⁶⁾ This theory is based on the non-Fermi liquid state in which the distinct excitations, spinon and holon, exist. In the RVB theory, the spinon pairing occurs at T^* (so-called 'spin gap'), and holons condense at T_c . Since 'spin gap' is based on the singlet pairing, the RVB theory explains the various experiments for under-doped cuprates. However, the continuities from the normal states to the superconducting states and from over-doped to under-doped cuprates are not necessarily obvious, and the physical origin of the spin-charge separation is not clear.

The magnetic scenarios based on the anti-ferromagnetic or SDW gap formation or their precursor have been proposed by various authors.^{17,18)} In these theories, 'hot spot', which is a part of the Fermi surface in the vicinity of the anti-ferromagnetic Brillouin zone, exists near $(0, \pi)$ and plays an especial role. Since the quasiparticles at 'hot spot' are strongly scattered by the anti-ferromagnetic spin fluctuations, the gap structure appears at 'hot spot'. However, considering that the ground state is actually superconductive, we can hardly expect that the magnetic order and the superconductivity are continuously connected beyond the superconducting transition. We shall give a discussion about this point in the last section.

Next, we describe the pairing scenarios based on the strong coupling superconductivity. Generally, the strong coupling superconductivity indicates the existence of the incoherent Cooper pairs (pre-formed pairs), as the famous Nozières and Schmitt-Rink formalism¹⁹⁾ has described. The strong attractive interaction produces the pre-formed pairs above the superconducting critical point. The pre-formed pairs condense at the critical point.

Our scenario in this paper is different from such a simple viewpoint. We think of the pseudogap as the phenomena brought about by the strong superconducting fluctuations. We actually carry out the different calculations from the Nozières and Schmitt-Rink formalism. The strong coupling superconductivity naturally gives rise to the strong fluctuations and the deviations from the BCS mean field descriptions. Because the short coherence length, which is attributed to the high critical temperature T_c compared with the renormalized Fermi energy $\tilde{\epsilon}_F$, and the quasi two-dimensionality characterize the superconductivity of High- T_c cuprates, it is natural to consider the strong superconducting fluctuations.

The strong coupling superconductivity has been discussed from the view point of the crossover from the BCS superconductivity to the Bose-Einstein condensation both in the ground state²⁰⁾ and at the finite temperature.¹⁹⁾ The concept of the Nozières and Schmitt-Rink formalism¹⁹⁾ is taking account of the corrections to the thermodynamic potential shown in Fig.1 and deciding the chemical potential self-consistently. This procedures correspond to counting the number of the bosonic pairs. Their formalism is justified in the low density limit. Several authors have discussed

the applicability of the Nozières and Schmitt-Rink formalism to the two-dimensional systems.^{21,22)}

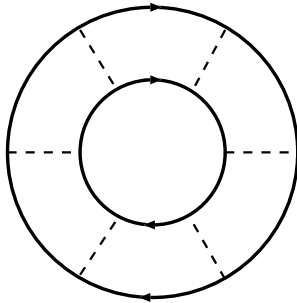


Fig. 1. The correction to the thermodynamic potential introduced in the Nozières and Schmitt-Rink theory.

The precursor of the superconductivity has been proposed for High- T_c cuprates by Randeria *et al.*²³⁾ on the basis of the functional integral formulation for s -wave symmetry. The Ginzburg-Landau theory is derived for d -wave symmetry by Stintzing and Zwerger.²⁴⁾ The self-consistent calculation has been carried out by Haussmann.²⁵⁾ Their theories have been based on the Nozières and Schmitt-Rink formalism¹⁹⁾ and treated the Fermi gas model or the low density model. The Nozières and Schmitt-Rink formalism has been applied to the $d - p$ model by Koikegami and Yamada.²⁶⁾

However, if anything, the nearly half-filled lattice system should be regarded as the rather high density system. Moreover, since the pseudogap phenomena take place near the Fermi surface, the situation in which the Fermi surface remarkably changes and disappears at last is not realistic. Therefore, we must take account of the higher order corrections in order to consider the effects of the superconducting fluctuations on the normal state electronic structure.

The phase fluctuation scenarios have been proposed by Emery and Kivelson,²⁷⁾ and calculated by other authors.²⁸⁾ The phenomenology based on the electron-like pre-formed pairs coexisting with unpaired fermions have been described by Geshkenbein *et al.*²⁹⁾ with reference to the sign problem of the fluctuational Hall effect. We shall shortly discuss the problem in the next section.

The explicit self-consistent T-matrix calculations for the electronic structure has been carried out numerically by several authors.^{30,31)} However, their calculations deal with somewhat unrealistic situations such as the low density, the particle-hole symmetry and so on. We shall point out the importance of their realistic factors later.

Maly *et al.*³²⁾ have introduced the idea of 'resonances' which means the scattering mechanism by

the presence of the meta-stable pre-formed pairs. We also adopt the idea in this paper. However, the approximation adopted by Maly *et al.*, in which one of the Green functions in the T-matrix is renormalized and the other is unrenormalized, is not natural, and the idea of 'resonances' is artificially introduced. Moreover, they have assumed the gap-like self-energy $\Sigma^R(\mathbf{k}, \omega) \propto \frac{1}{\omega + \varepsilon_{\mathbf{k}} + i\Gamma_0}$. Their assumption is not self-evident for the self-consistent calculation and should be confirmed explicitly. Actually, we shall show later that their assumption cannot satisfy the self-consistency.

In this paper, on the basis of the strong coupling superconductivity, we make a fully self-consistent calculation to derive the character of the superconducting fluctuations as the weakly-damped pre-formed pairs and explicitly calculate the single particle self-energy.

This paper is constructed as follows. In §2, we give a model Hamiltonian and explain the basic formalism adopted in this paper. In §3 and §4, we explicitly calculate the single particle self-energy corresponding to the T-matrix and the self-consistent T-matrix approximations, respectively. In §5, we summarize the obtained results and give discussions on the several related issues.

§2. Basic Formalism

In this section we describe the basic formalism for the idea of the resonances of quasiparticles with the thermally excited weakly-damped pre-formed pairs on the basis of the time-dependent-Ginzburg-Landau (TDGL) expansion for the superconducting pairing fluctuations. The pairing fluctuations have essentially different properties in the strong coupling case from those in the weak coupling limit. We show that the strong coupling superconductivity leads to the anomalous normal state properties above the superconducting critical temperature. Hereafter, we adopt the unit $\hbar = c = k_B = 1$.

We introduce the following two-dimensional model Hamiltonian which has a $d_{x^2-y^2}$ -wave superconducting ground state, with High- T_c cuprates in mind.

$$H = \sum_{\mathbf{k}, s} \varepsilon_{\mathbf{k}} c_{\mathbf{k}, s}^\dagger c_{\mathbf{k}, s} + \sum_{\mathbf{k}, \mathbf{k}', \mathbf{q}} V_{\mathbf{k}-\mathbf{q}/2, \mathbf{k}'-\mathbf{q}/2} c_{\mathbf{k}', \uparrow}^\dagger c_{\mathbf{q}-\mathbf{k}', \downarrow}^\dagger c_{\mathbf{k}, \uparrow} c_{\mathbf{q}-\mathbf{k}, \downarrow}, \quad (2.1)$$

where $V_{\mathbf{k}, \mathbf{k}'}$ is the $d_{x^2-y^2}$ -wave separable pairing interaction,

$$V_{\mathbf{k}, \mathbf{k}'} = g \varphi_{\mathbf{k}} \varphi_{\mathbf{k}'}, \quad (2.2)$$

$$\varphi_{\mathbf{k}} = \cos k_x - \cos k_y, \quad (2.3)$$

where g is negative. $\varphi_{\mathbf{k}}$ is the $d_{x^2-y^2}$ -wave form factor, and it is a constant value for the conventional s -wave case.

We consider the dispersion $\varepsilon_{\mathbf{k}}$ given by the tight-binding model for a square lattice including the nearest- and next-nearest-neighbor hopping t, t' , respectively,

$$\varepsilon_{\mathbf{k}} = -2t(\cos k_x + \cos k_y) + 4t' \cos k_x \cos k_y - \mu. \quad (2.4)$$

We fix the lattice constant $a = 1$. We adopt $t = 0.5\text{eV}$ and $t' = 0.45t$. These parameters reproduce the Fermi surface of the typical High- T_c cuprates, $\text{YBa}_2\text{Cu}_3\text{O}_{6+\delta}$ and $\text{Bi}_2\text{Sr}_2\text{CaCu}_2\text{O}_{8+\delta}$. We choose the chemical potential μ so that the filling $n = 0.9$. This filling corresponds to the hole doping $\delta = 0.1$. The Fermi surface is shown in Fig.2.

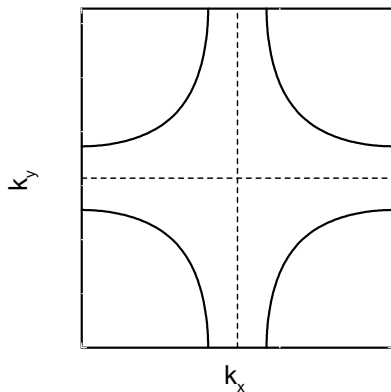


Fig. 2. The Fermi surface adopted in this paper.

Since the Brillouin zone edge acts as a natural momentum cut-off, we do not have to use the renormalization methods in order to remove the ultraviolet divergences which exist in the Fermi gas model.²³⁾

In reality, the origin of the pairing interaction should be considered to be the anti-ferromagnetic spin fluctuations. The spin fluctuations not only cause the pairing interaction but also affect the electronic state such as the momentum dependent lifetime, the momentum dependent mass enhancement and so on.⁹⁾ There are studies dealing with the pairing correlations obtained by the spin fluctuations on the basis of the fluctuation exchange (FLEX) approximation.^{33,34)} However, we do not positively adopt these effects because we think that these details do not qualitatively affect the pseudogap phenomena as a precursor of the $d_{x^2-y^2}$ -wave superconductivity. Indeed, from both a theory of the transport phenomena⁹⁾ and the NMR experiments,^{2,3)} it should be considered that the low frequency component of the anti-ferromagnetic spin fluctuations is suppressed in the pseudogap

region. The electronic state is mainly affected by the low frequency component. Moreover, this suppression does not contradict with our assumption that the pairing interaction is not suppressed in the pseudogap region, because the pairing interaction is mainly caused by the high frequency component of the spin fluctuations.

First of all, we consider the properties of the scattering vertex arising from the superconducting fluctuations, $\Gamma(\mathbf{k}, \mathbf{q} - \mathbf{k} : \mathbf{k}', \mathbf{q} - \mathbf{k}' : i\Omega_n)$. The vertex is described by the ladder diagrams (T-matrix) in the particle-particle interaction channel as shown in Fig.3.

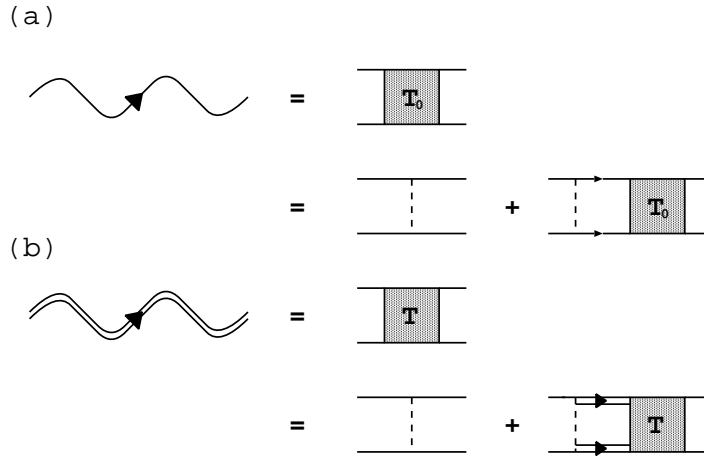


Fig. 3. The scattering vertex represented by the ladder diagrams in the particle-particle channel (T-matrix). The dashed lines represent the attractive interaction. The single and double solid lines represent the propagators of the bare and renormalized fermions, respectively. The single and double wavy lines represent the propagators of the bare and renormalized fluctuating Cooper pairs, respectively.

It is factorized into $\Gamma(\mathbf{k}, \mathbf{q} - \mathbf{k} : \mathbf{k}', \mathbf{q} - \mathbf{k}' : i\Omega_n) = \varphi_{\mathbf{k}-\mathbf{q}/2} t(\mathbf{q}, i\Omega_n) \varphi_{\mathbf{k}'-\mathbf{q}/2}$, where

$$\begin{aligned}
 t(\mathbf{q}, i\Omega_n)^{-1} &= g^{-1} + \chi_0(\mathbf{q}, i\Omega_n), \\
 \chi_0(\mathbf{q}, i\Omega_n) &= T \sum_{\mathbf{k}', \omega_m} G(\mathbf{k}', i\omega_m) G(\mathbf{q} - \mathbf{k}', i\Omega_n - i\omega_m) \varphi_{\mathbf{k}'-\mathbf{q}/2}^2.
 \end{aligned} \tag{2.5}$$

Here, $\omega_m = 2\pi(m + \frac{1}{2})T$ and $\Omega_n = 2\pi nT$ are the fermionic and bosonic Matsubara frequencies, respectively.

As a result of the analytic continuation, $\chi_0(\mathbf{q}, \Omega)$ is expressed as

$$\chi_0^{\text{R}}(\mathbf{q}, \Omega) = \sum_{\mathbf{k}} \int \frac{d\omega}{\pi} [f(\omega - \Omega) \text{Im} G^{\text{R}}(\mathbf{q} - \mathbf{k}, \Omega - \omega) G^{\text{R}}(\mathbf{k}, \omega) - f(\omega) G^{\text{R}}(\mathbf{q} - \mathbf{k}, \Omega - \omega) \text{Im} G^{\text{R}}(\mathbf{k}, \omega)] \varphi_{\mathbf{k}-\mathbf{q}/2}^2. \quad (2.6)$$

Here, $Z_{sc} = (1 + g\chi_0(\mathbf{q}, \Omega))^{-1}$ is regarded as an enhancement factor for the superconducting susceptibility $\chi_{sc}(\mathbf{q}, \Omega)$. When $1 + g\chi_0(\mathbf{0}, 0) = 0$, $\chi_{sc}(\mathbf{0}, 0)$ diverges and the superconductivity occurs. This is the famous Thouless criterion which is equivalent to the BCS theory in the weak coupling limit.¹⁹⁾

$t(\mathbf{q}, \Omega)$ can be regarded as a propagator of the fluctuating Cooper pairs. The Thouless criterion corresponds to the situation in which $t(\mathbf{q}, \Omega)$ has its pole at $\mathbf{q} = \Omega = 0$.

Here, we are interested in the normal state near the superconducting critical point, where the Z_{sc} grows and the superconducting fluctuations are strongly enhanced. Even in the weak coupling limit, this divergence affects the various physical quantities,^{35, 36)} and the several studies based on such a framework have been given for High- T_c cuprates.³⁷⁻⁴²⁾ However, in the strong or intermediate coupling region, the superconducting fluctuations more seriously affect the electronic states. We will show that below.

Because $t(\mathbf{q}, \Omega)$ is strongly enhanced at $\mathbf{q} = \Omega = 0$ near the superconducting critical point, its contribution to the single particle self-energy $\Sigma(\mathbf{k}, \omega)$ is mainly from the vicinity of $\mathbf{q} = \Omega = 0$. Therefore, we expand $t^{-1}(\mathbf{q}, \Omega)$ in the vicinity of $\mathbf{q} = \Omega = 0$.

We describe the expansion as follows,

$$gt^{-1}(\mathbf{q}, \Omega) = t_0 + b\mathbf{q}^2 - (a_1 + ia_2)\Omega. \quad (2.7)$$

This expansion corresponds to the time-dependent-Ginzburg-Landau (TDGL) expansion up to the second order. In the above description, $t_0 = 1 + \chi_0(\mathbf{0}, 0)$. The other parameters b , $a_1 + ia_2$ are expressed by the differentiation of $\chi_0(\mathbf{q}, \Omega)$ with respect to the momentum and frequency, respectively.

Later, we explicitly estimate $\chi_0(\mathbf{q}, \Omega)$ and the TDGL expansion parameters, for the non-interacting Green function (bare Green function) $G^{\text{R}(0)}(\mathbf{k}, \omega) = (\omega - \varepsilon_{\mathbf{k}} + i\delta)^{-1}$ in §3, and for the renormalized Green function $G^{\text{R}}(\mathbf{k}, \omega) = (\omega - \varepsilon_{\mathbf{k}} - \Sigma^{\text{R}}(\mathbf{k}, \omega))^{-1}$ in §4, respectively.

These estimations correspond to the T-matrix approximation (see Fig.4(a)) and the self-consistent T-matrix approximation (see Fig.4(b)) for the single particle self-energy, respectively. We carry out the explicit calculation in the following sections.

In this section, we give an account of the general properties of the TDGL parameters, and phenomenologically calculate the contribution of the superconducting fluctuations to the single particle self-energy.

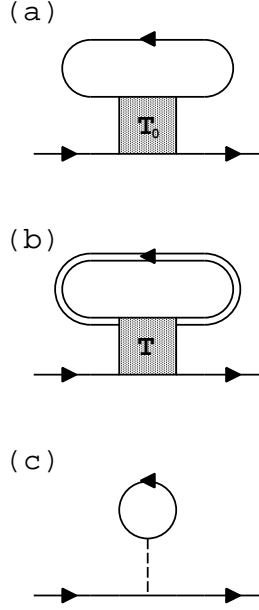


Fig. 4. The diagrams of the single particle self-energy based on (a) the T-matrix approximation and (b) the self-consistent T-matrix approximation, respectively. (c) The Hartree-Fock term which we exclude afterward. We consider that this term is included in the dispersion relation $\varepsilon_{\mathbf{k}}$ from the beginning.

First, we describe the expression in the weak coupling limit. In this case, we can use the bare Green function $G^{R(0)}$. $\chi_0(\mathbf{q}, \Omega)$ is expressed as follows:

$$\chi_0(\mathbf{q}, \Omega) = \sum_{\mathbf{k}} \frac{1 - f(\varepsilon_{\mathbf{k}+\mathbf{q}/2}) - f(\varepsilon_{-\mathbf{k}+\mathbf{q}/2})}{\varepsilon_{\mathbf{k}+\mathbf{q}/2} + \varepsilon_{-\mathbf{k}+\mathbf{q}/2} - \Omega} \varphi_{\mathbf{k}}^2, \quad (2.8)$$

where, $f(\varepsilon)$ is the Fermi distribution function. Therefore, the parameters are expressed as follows:

$$\begin{aligned} t_0 &= 1 + g \int d\varepsilon \frac{\tanh(\frac{\varepsilon}{2T})}{2\varepsilon} \rho_d(\varepsilon) \cong |g| \rho_d(0) \frac{T - T_c}{T_c}, \\ b &= |g| \int d\varepsilon \frac{\rho_d(\varepsilon) \bar{v}_F^2}{16\varepsilon} \frac{\partial^2 f(\varepsilon)}{\partial \varepsilon^2} \cong |g| \rho_d(0) \frac{7\zeta(3)}{32(\pi T)^2} \bar{v}_F^2, \\ a_1 &= |g| \int d\varepsilon \frac{\tanh(\frac{\varepsilon}{2T})}{(2\varepsilon)^2} \rho_d(\varepsilon), \\ a_2 &= |g| \rho_d(0) \frac{\pi}{8T}, \end{aligned} \quad (2.9)$$

where $\zeta(3)$ is the Riemann's zeta function and \bar{v}_F is the mean value of the quasiparticle's velocity on the Fermi surface. Here, we have defined the effective density of states for the $d_{x^2-y^2}$ -wave symmetry.

$$\rho_d(\varepsilon) = \sum_{\mathbf{k}} \rho_{\mathbf{k}}(\varepsilon) \varphi_{\mathbf{k}}^2, \quad (2.10)$$

where, $\rho_{\mathbf{k}}(\varepsilon)$ is the spectral weight $\rho_{\mathbf{k}}(\varepsilon) = A_{\mathbf{k}}(\varepsilon) = -\frac{1}{\pi} \text{Im} G^R(\mathbf{k}, \omega)$.

It should be noticed that $\rho_d(\varepsilon)$ is more sensitive to the pseudogap formation rather than the density of states $\rho(\varepsilon) = \sum_{\mathbf{k}} \rho_{\mathbf{k}}(\varepsilon)$. Because of the $d_{x^2-y^2}$ -wave-like pseudogap formation, the quasiparticle peak vanishes in the vicinity of $(\pi, 0)$ where the form factor $\varphi_{\mathbf{k}}$ is large. Although the quasiparticle peak remains in the vicinity of $(\pi/2, \pi/2)$, this area contributes little to $\rho_d(\varepsilon)$ because of the form factor $\varphi_{\mathbf{k}}$. Therefore, the pseudogap formation remarkably suppresses $\rho_d(\varepsilon)$. In this sense, the difference between the s -wave and the d -wave is small.

The parameter b is generally related to the coherence length ξ , $b \propto \xi^2$, and is very large in the weak coupling limit. As the coupling becomes stronger and the critical temperature increases, b decreases. Moreover, the pseudogap formation decreases b . In this case, which means the short coherence length superconductor, the superconducting fluctuations become notable.

Generally, $a_1 = 0$ for the particle-hole symmetric case. However, it is non-zero in the realistic asymmetric systems. The general expression for a_1 has been given by Ebisawa and Fukuyama.⁴³⁾ Following them, we obtain

$$a_1 \propto \left. \frac{\partial \rho_d(\varepsilon)}{\partial \varepsilon} \right|_{\varepsilon=0}. \quad (2.11)$$

This quantity has been related to the Hall coefficient in the superconducting critical region.⁴⁴⁾ It has been pointed out⁴⁵⁾ that the sign-reversal of the Hall coefficient under the high magnetic fields for High- T_c cuprates is not consistent with the above general expression.

In the weak coupling limit, a_1 is higher order than a_2 with respect to the small parameter T_c/ε_F . Therefore, a_1 is usually neglected except for the Hall coefficient. However, a_1 should not be neglected for High- T_c cuprates which is expected to be in the intermediate or strong coupling region, because T_c/ε_F increases with the coupling constant $|g|$.

Furthermore, when the pseudogap opens, a_2 remarkably decreases because of the suppression of the effective density of states $\rho_d(0)$. On the other hand, the pseudogap formation does not have much effect on a_1 , because there is the same order contribution to a_1 from the high energy part as well as from the low energy part considered by Ebisawa and Fukuyama (eq. 2.11). The expression by Ebisawa and Fukuyama is justified for the pairing interaction by the electron-phonon mechanism in which the pairing interaction is restricted to the vicinity of the Fermi surface. For

High- T_c cuprates, however, the pairing interaction is not restricted so because of the non-electron-phonon mechanism. Therefore, there exists the contribution from the high energy part. For High- T_c cuprates, the contribution from the high energy part is mainly from the vicinity of the Van Hove singularity at $(\pi, 0)$, and has the same sign as that from the low energy part. It is not affected by the pseudogap formation. Therefore, a_1 is not so greatly reduced by the pseudogap formation, and we must precisely estimate a_1 using eq. 2.6.

As a result of the above discussion, we expect that the condition $|a_1| \geq a_2$ is realized near the superconducting critical point in the intermediate or strong coupling case. This expectation is confirmed by our explicit self-consistent calculation in §4. This expectation means that the fluctuating Cooper pairs become propagative and obtain the character of the pre-formed pairs, although they are over-damped diffusive mode in the conventional weak coupling theory.

It should be noticed that the sign of a_1 depends on the band structure. For High- T_c cuprates, a_1 is negative. This fact indicates that the pre-formed pairs are hole-like in High- T_c cuprates.

Geshkenbein *et al.* phenomenologically assumed that the pre-formed pairs are electron-like in order to explain the sign problem of the fluctuational Hall coefficient.²⁹⁾ However, even in the strong coupling region, the sign of a_1 is negative and the pre-formed pairs are hole-like. Therefore, we think that the assumption by Geshkenbein *et al.* is broken. We consider that the simple strong coupling scenario cannot explain the sign problem.

In the remaining part of this section, we calculate the single particle self-energy corresponding to the one-loop diagram (Fig.5(a)) on the basis of the above TDGL expansion for the T-matrix. Here, we phenomenologically define the TDGL parameters and use the bare Green function for simplicity. Hereafter, we choose t_0 as a small parameter. Therefore, our theory is an approach starting from the actual superconducting critical point.

The self-energy is given by

$$\Sigma(\mathbf{k}, i\omega_n) = T \sum_{\mathbf{q}, i\Omega_m} t(\mathbf{q}, i\Omega_m) G(\mathbf{q} - \mathbf{k}, i\Omega_m - i\omega_n) \varphi_{\mathbf{k}-\mathbf{q}/2}^2. \quad (2.12)$$

After the analytic continuation, we obtain

$$\begin{aligned} \Sigma^R(\mathbf{k}, \omega) &= \sum_{\mathbf{q}} \int \frac{d\Omega}{\pi} [b(\Omega) \text{Im}t(\mathbf{q}, \Omega) G^A(\mathbf{q} - \mathbf{k}, \Omega - \omega) - f(\Omega) t(\mathbf{q}, \Omega + \omega) \text{Im}G^R(\mathbf{q} - \mathbf{k}, \Omega)] \varphi_{\mathbf{k}-\mathbf{q}/2}^2, \\ \text{Im}\Sigma^R(\mathbf{k}, \omega) &= - \sum_{\mathbf{q}} \int \frac{d\Omega}{\pi} [b(\Omega + \omega) + f(\Omega)] \text{Im}t(\mathbf{q}, \Omega + \omega) \text{Im}G^R(\mathbf{q} - \mathbf{k}, \Omega) \varphi_{\mathbf{k}-\mathbf{q}/2}^2, \end{aligned} \quad (2.13)$$

where $b(\Omega)$ is the Bose distribution function. In the conventional Fermi liquid theory, the factor $[b(\Omega + \omega) + f(\Omega)]$ gives the common relation $\text{Im}\Sigma^R(\mathbf{k}, \omega) \propto \omega^2 + (\pi T)^2$. However, when the strong

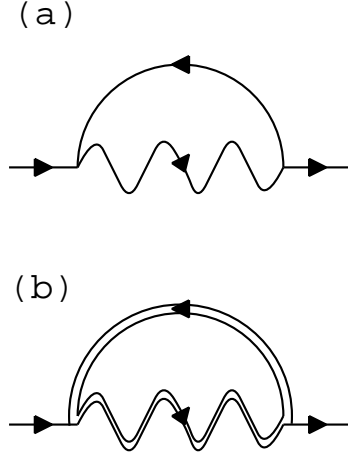


Fig. 5. The single particle self-energy of the one-loop diagram. The wavy lines represent the propagator of the fluctuating Cooper pairs described by the TDGL parameters. Fig.5(a) and Fig.5(b) correspond to Fig.4(a) and Fig.4(b), respectively.

fluctuations exist, the strong \mathbf{q} - and Ω -dependence of $t(\mathbf{q}, \Omega)$ give rise to the anomalous features as we show below.

Assuming $|a_1| \gg a_2$, we describe the imaginary part of the T-matrix as

$$\text{Im}t(\mathbf{q}, \Omega) = g \frac{\pi}{a_1} \delta(\Omega - \Omega_{\mathbf{q}}) \quad (2.14)$$

Here, we have defined $\Omega_{\mathbf{q}} = (t_0 + b\mathbf{q}^2)/a_1$. This quantity corresponds to the dispersion relation of the pre-formed pairs. Because a_1 is negative in our case, $\Omega_{\mathbf{q}} < 0$. Therefore, the pre-formed pairs have not electron-like but hole-like character.

Substituting eq. 2.14 into eq. 2.13, we obtain

$$\begin{aligned} \text{Re}\Sigma^{\text{R}}(\mathbf{k}, \omega) &= \sum_{\mathbf{q}} g \left[\frac{1}{a_1} b(\Omega_{\mathbf{q}}) \text{Re}G^{\text{R}}(\mathbf{q} - \mathbf{k}, \Omega_{\mathbf{q}} - \omega) \right. \\ &\quad \left. - \int \frac{d\Omega}{\pi} f(\Omega - \omega) \frac{1}{t_0 + b\mathbf{q}^2 - a_1\Omega} \text{Im}G^{\text{R}}(\mathbf{q} - \mathbf{k}, \Omega - \omega) \right] \varphi_{\mathbf{k}-\mathbf{q}/2}^2, \\ \text{Im}\Sigma^{\text{R}}(\mathbf{k}, \omega) &= - \sum_{\mathbf{q}} \frac{g}{a_1} [b(\Omega_{\mathbf{q}}) + f(\Omega_{\mathbf{q}} - \omega)] \text{Im}G^{\text{R}}(\mathbf{q} - \mathbf{k}, \Omega_{\mathbf{q}} - \omega) \varphi_{\mathbf{k}-\mathbf{q}/2}^2. \end{aligned} \quad (2.15)$$

We can see from the above expressions that the singular contribution in the small t_0 limit arises from the terms proportional to $b(\Omega_{\mathbf{q}})$. Therefore, we estimate the singular terms for the linearized

bare Green function $G^{(0)\text{R}}(\mathbf{q} - \mathbf{k}, \omega) = (\omega - \varepsilon_{\mathbf{k}} + v_{\mathbf{k}}\mathbf{q} + i\delta)^{-1}$. Because the singular contribution arises from the vicinity of $\mathbf{q} = 0$, we restrict the \mathbf{q} -sum to the region $|\Omega\mathbf{q}| \leq T$, and use the approximate relation $b(\Omega\mathbf{q}) \sim \frac{T}{\Omega\mathbf{q}}$. Since only the small region in the vicinity of $\mathbf{q} = 0$ contributes to the self-energy, we can neglect the \mathbf{q} -dependence of the form factor $\varphi_{\mathbf{k}-\mathbf{q}/2}$. We exactly calculate the \mathbf{q} -sum. However, the results are very complicated. Therefore, we show the approximate results as follows

$$\text{Re}\Sigma^{\text{R}}(\mathbf{k}, \omega) = \begin{cases} -g\varphi_{\mathbf{k}}^2 \frac{T}{4\pi b} \frac{1}{\alpha} \log\left[\frac{a_1}{t_0} \min(T, \alpha, \alpha^2 b/|a_1|v_{\mathbf{k}}^2)\right] & (|\alpha| \gg \frac{t_0}{|a_1|}) \\ -g\varphi_{\mathbf{k}}^2 \frac{T}{2\pi a_1 v_{\mathbf{k}}^2} \left(\frac{a_1}{t_0} \alpha - 1\right) & (|\alpha| \sim \frac{t_0}{|a_1|}), \end{cases} \quad (2.16)$$

$$\text{Im}\Sigma^{\text{R}}(\mathbf{k}, \omega) = \begin{cases} g\varphi_{\mathbf{k}}^2 \frac{T}{4b} (\alpha^2 + \frac{v_{\mathbf{k}}^2}{b} t_0)^{-\frac{1}{2}} & (|\alpha| \leq T) \\ 0 & (\alpha \geq \frac{|a_1|v_{\mathbf{k}}^2}{4b} - \frac{t_0}{|a_1|}), \end{cases} \quad (2.17)$$

where we have defined $\alpha = \omega + \varepsilon_{\mathbf{k}}$.

We show the typical features of $\text{Re}\Sigma^{\text{R}}(\mathbf{k}, \omega)$, $\text{Im}\Sigma^{\text{R}}(\mathbf{k}, \omega)$ and $\pi A(\mathbf{k}, \omega) = -\text{Im}G^{\text{R}}(\mathbf{k}, \omega)$ in Fig.6.

It is notable that the real part of the self-energy has the positive slope in the vicinity of $\alpha = 0$, and the imaginary part of the self-energy has the sharp peak at $\alpha = 0$ in its absolute value. The both features are anomalous compared with the conventional Fermi liquid theory. These anomalous features of the single particle self-energy should be regarded as the effects of the resonances of quasiparticles with the weakly-damped thermally excited pre-formed pairs. Such drastic phenomena take place on the condition $|\Omega\mathbf{0}| \ll T$. Of course, the characteristics of the strong coupling superconductivity are reflected on the properties of the TDGL parameters. As the coupling constant $|g|$ increases and the critical temperature increases, the effects of the resonances become remarkable.

Although we have used the assumption $|a_1| \gg a_2$ in the above analytic calculation, the results change little even in the more gentle condition $|a_1| \sim a_2$. Furthermore, these features do not change qualitatively even in the strongly diffusive region $|a_1| \ll a_2$. However, the absolute value of the self-energy is considerably small in the diffusive case. Therefore, these effects are very small in the weak coupling case.

It should be noticed that the self-energy essentially has the asymmetric structure, which naturally arises from the hole-like features of the pre-formed pairs. In particular, the imaginary part has the long tail on the negative frequency side.

Norman *et al.*⁴⁶⁾ have used the assumption $\Sigma^{\text{R}}(\mathbf{k}, \omega) \propto \frac{1}{\omega + \varepsilon_{\mathbf{k}} + i\Gamma_0}$ in order to explain the data of the ARPES experiments. Our results are qualitatively consistent with their assumption. However, we shall point out in §4 that the slight break down of the assumption which originates from the asymmetric structure is important for the self-consistent solution.

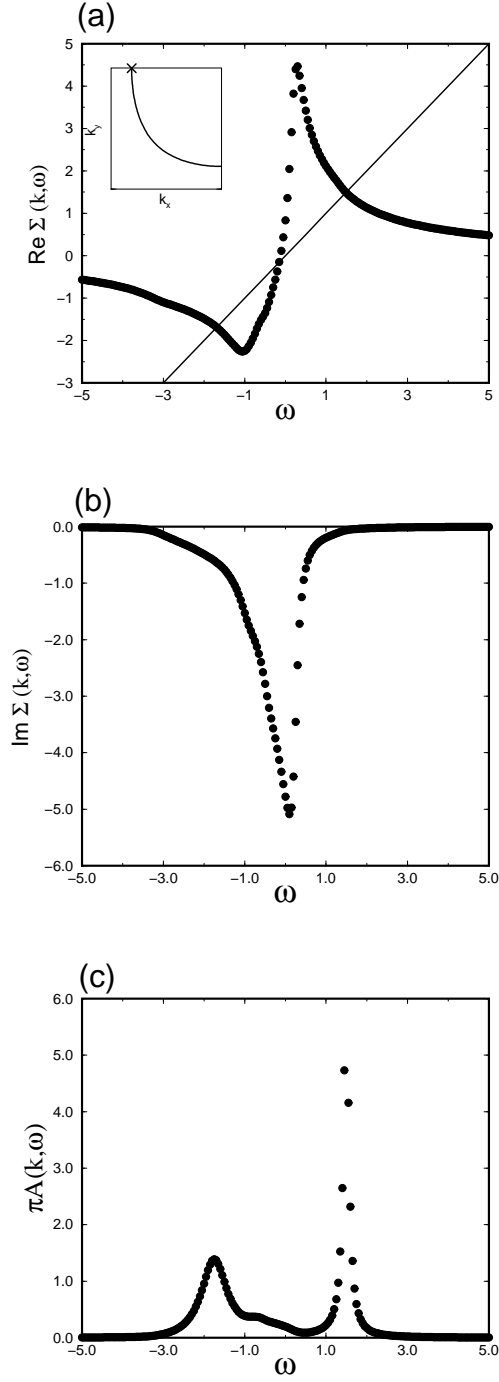


Fig. 6. (a) The real part of the self-energy given by the one loop diagram in Fig.5(a). The solid line shows the condition $\omega - \varepsilon_{\mathbf{k}} - \text{Re} \Sigma^{\text{R}}(\mathbf{k}, \omega) = 0$. (b) The imaginary part of the self-energy. (c) The spectral weight. For all figures, the \mathbf{k} -point is chosen on the Fermi surface near $(0, \pi)$. (see inset in (a)). Here, the coupling constant and the TDGL parameters are phenomenologically chosen as $g = -2.0$, $a_1 = -1.0$, $a_2 = 0.2$, $b = 0.2$, $t_0 = 0.03$, $T = 0.2$.

The quantity $A(\mathbf{k}, \omega)$ corresponds to the spectral weight. According to Fig.6(a), there are three solutions of the equation $\omega - \varepsilon_{\mathbf{k}} - \text{Re}\Sigma^{\text{R}}(\mathbf{k}, \omega) = 0$. However, since the imaginary part of the self-energy is extremely large in the vicinity of $\alpha = 0$, the middle solution in Fig.6(a) disappears. Therefore, the spectral weight has the gap-like two peak structure at

$$E = \pm \sqrt{\varepsilon_{\mathbf{k}}^2 + \Delta_{\mathbf{k}}^2}, \quad (2.18)$$

$$\Delta_{\mathbf{k}}^2 = |g|\varphi_{\mathbf{k}}^2 \frac{T}{4\pi b} \log\left[\frac{T}{a_1}\right]. \quad (2.19)$$

This spectrum is similar to that of the conventional superconducting state. Although the gap amplitude is related to the condensed Cooper pairs in the superconducting state, here, $\Delta_{\mathbf{k}}^2$ is proportional to the number of the thermally excited pre-formed pairs $n_{\text{B}} \propto \sum_{\mathbf{q}} b(\Omega_{\mathbf{q}})$.

Furthermore, the spectral weight also has the asymmetric structure. The spectrum has the relatively broad peak on the negative frequency side and the sharp peak on the positive frequency side. Randeria *et al.*⁴⁷⁾ have proposed the assumption of the particle-hole symmetry for the spectral weight, and actually Norman *et al.*¹¹⁾ carried out the analysis for the ARPES data on the basis of the assumption. We consider that this analysis is not so wrong qualitatively. However, our calculation shows that this assumption is essentially broken reflecting the hole-like character of the pre-formed pairs. Indeed, the asymmetry plays an important role in the self-consistent calculation in §4.

We shall numerically carry out the explicit calculation for the TDGL parameters and the single-particle self-energy corresponding to the T-matrix (in §3) and the self-consistent T-matrix (in §4) approximations in the following sections.

It is notable that the effects of the resonances described above are extraordinary small and can not be seen in the weak coupling limit, where b is large and $|a_1| \ll a_2$ because of the small T_c . Therefore, the effects of the resonances are the characteristics of the strong coupling superconductivity.

However, as we described above, the anomalous features, such as the relatively large imaginary part of the self-energy in the vicinity of $\alpha = 0$ and so on, exist even in the weak coupling case. Consequently, the density of states at the Fermi level are slightly suppressed even in the weak coupling case. This effect has already been discussed by the other authors on the basis of the conventional weak coupling formalism.³⁸⁻⁴²⁾ In particular, Eschrig *et al.*⁴²⁾ have shown that the NMR experiments for the optimally-doped cuprates are understood on the basis of the conventional d -wave superconducting fluctuation theory. Also in their theory, the suppression of the density of states plays an essential role. This effect appears also in our theory. However, it is more remarkable and leads to the gap-like structure of the spectral weight in the strong coupling case. In this sense, our theory is a natural extension of these conventional weak coupling theories.

It should be noticed that there is a logarithmic singularity of the self-energy and $\Delta_{\mathbf{k}}$ near the

critical point, reflecting the singularity of two-dimensional systems. Strictly speaking, it leads to the fact $T_c = 0$. This is a natural result which satisfies the Marmin-Wagner's theorem. The Nozières and Schmitt-Rink formalism for two-dimensional systems^{21,22)} has the similar singularity, and the critical temperature $T_c = 0$.

However, we consider that there is not such a singularity in the realistic layered systems. Although the quasi-two-dimensionality enhances the effects of the fluctuations in the layered systems, the weak three-dimensionality is sure to remove the singularity.³⁹⁾

Here, we comment on the Nozières and Schmitt-Rink formalism. The Nozières and Schmitt-Rink theory takes account of the shift of the chemical potential by the creation of the bosonic particles, and decides the critical temperature T_c using the Thouless criterion for the shifted chemical potential. It should be noticed that for High- T_c cuprates the chemical potential shifts upward because the pre-formed pairs are not electron-like, but hole-like. It is the opposite direction compared to the Fermi gas model or the low density lattice model. (see Fig. 7.) The upward shift seems to be natural because the density of states decreases in that direction.

This formalism is justified in the low density limit. However, High- T_c cuprates should be regarded as rather high density limit, because they are the lattice systems near the half-filling. Therefore, we need the extended calculation as is carried out in this paper.

In the low density limit, a strong attractive interaction easily creates the bosonic pre-formed pairs which can move almost freely, and the chemical potential shifts remarkably. There may be no serious effect on the normal state fermion system except for the chemical potential shift. This insight is suggested by the fact that the self-energy calculated in this section is proportional to n_B in rough estimate. n_B can not become so large in the low density systems. Therefore, the effects of the resonances described above cannot be seen in the low density limit. On the other hand, in high density systems, the effects of the resonances occur in the fermion systems before the chemical potential shifts remarkably. Therefore, although the chemical potential actually shifts also in the high density systems, the shift is not a dominant effect. The chemical potential shift is included in our calculation. However, we will not pay attention to it in the following sections.

§3. Lowest Order Calculation

In this section we explicitly calculate the single particle self-energy on the basis of the formalism described in the previous section.

First, we calculate the T-matrix around $\mathbf{q} = \Omega = 0$, for the non-interacting Green function $G^{R(0)}(\mathbf{k}, \omega) = (\omega - \varepsilon_{\mathbf{k}} + i\delta)^{-1}$, using eq. 2.6. We expand the reciprocal of the T-matrix, $t(\mathbf{q}, \Omega)^{-1}$ and estimate the TDGL expansion parameters. Of course, the results are equivalent to eq. 2.9.

Secondly, we calculate the single particle self-energy corresponding to the diagram shown in Fig.5(a), using eq. 2.13. This calculation corresponds to the T-matrix approximation (Fig.4(a)).

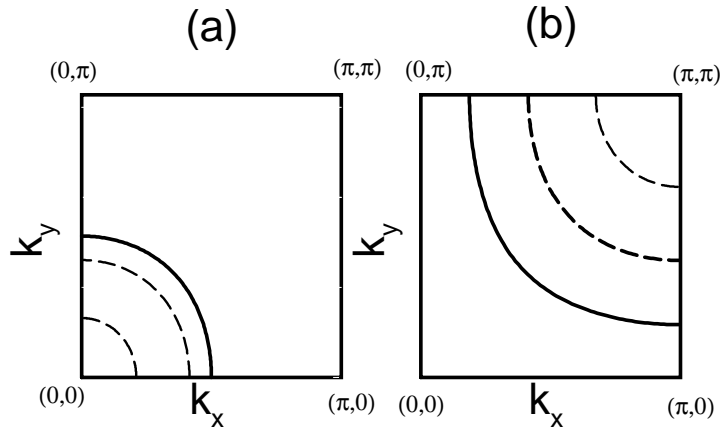


Fig. 7. The schematic figures of the transformation of the Fermi surface by the chemical potential shift based on the Nozières and Schmitt-Rink theory. The solid line shows the original Fermi surface, and the long-dashed line shows the shifted Fermi surfaces. (a) The case of the Fermi gas model, or the low density lattice model. The chemical potential shifts downward. (b) The case of High- T_c cuprates. The chemical potential shifts upward. This upward shift reflects the hole-like properties of the pre-formed pairs in High- T_c cuprates.

We exclude the trivial Hartree-Fock term corresponding to the diagram shown in Fig.4(c). We consider that this term is included in the dispersion relation $\varepsilon_{\mathbf{k}}$ from the beginning. This exclusion makes no difference in the strongly fluctuating region.

Because we use the non-interacting Green function, the superconducting critical temperature T_c is the same as that obtained by the BCS mean field theory, T_{MF} . Therefore, our calculation in this section is carried out above T_{MF} .

We show the results in Fig.8.

The self-energy shows the same features as we have calculated analytically in §2. Although $|a_1| \leq a_2$ is always realized in this calculation, the effects of the resonances clearly appear.

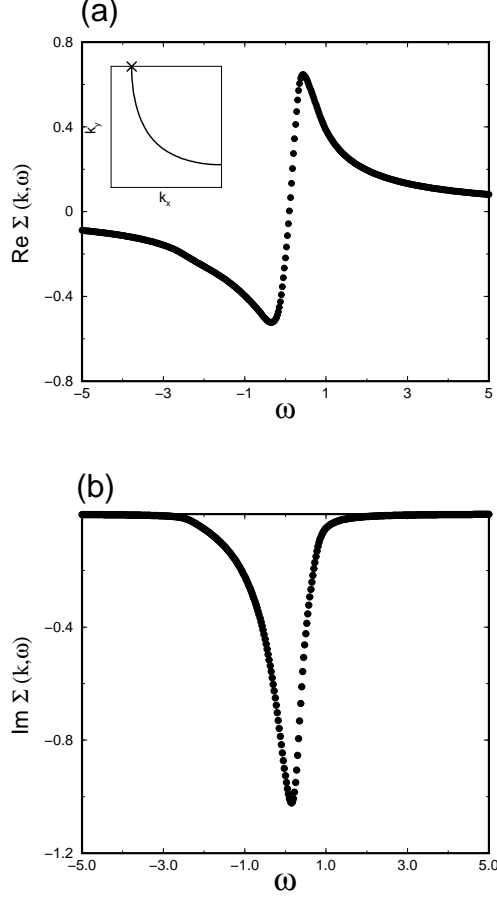


Fig. 8. The single particle self-energy on the Fermi surface near $(0, \pi)$ obtained by the lowest order calculation. (a)The real part. (b)The imaginary part. Here, $\mathbf{k} = (0.589, \pi)$, $g = -1.0$, and $T = 0.21$. The \mathbf{k} -point is shown in the inset. Here, $T_c = T_{\text{MF}} = 0.185$.

The spectral weight is shown in Fig.9 for various temperatures.

The spectral weight has the clear double peak gap-like structure in the low temperature region. As the temperature increases, the gap structure is filled up. Thus, the quasiparticle feature of the normal Fermi liquid theory realized at the higher temperature becomes unstable near the superconducting transition temperature $T_c = T_{\text{MF}} = 0.185$, where the superconducting fluctuations are strong. As a result, the resonance effects produce the gap-like double peak structure.

The momentum dependence of the spectral weight is shown in Fig.10.

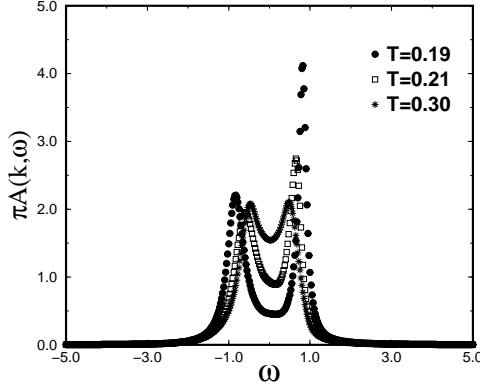


Fig. 9. The spectral weight for various temperatures $T = 0.19$ (circles), $T = 0.21$ (squares), $T = 0.30$ (stars). The other parameters are the same as those in Fig.8.

We can see that the amplitude of the gap is large in the vicinity of $(0, \pi)$, and decreases as the momentum approaches $(\pi/2, \pi/2)$. Furthermore, the single peak structure of quasiparticles exists in the vicinity of $(\pi/2, \pi/2)$. These features are consistent with the ARPES experiments.¹¹⁾ It is mainly because of the $d_{x^2-y^2}$ -wave form factor $\varphi_{\mathbf{k}}$. Thus, it is naturally led from our formalism that the pseudogap has the same shape as that of the superconducting gap. Since the attractive interaction is small in the vicinity of $(\pi/2, \pi/2)$, quasiparticles are not strongly affected there by the superconducting fluctuations.

The density of states $\rho(\varepsilon)$ is shown in Fig.11.

We calculate the self-energy only for the \mathbf{k} -points in the vicinity of the Fermi surface. Because the quasiparticles far from the Fermi surface are not so much affected by the superconducting fluctuations, we do not pay attention to them. We show the density of states in Fig.11, obtained by summing up the momentum on the calculated area. Therefore, the peak position is artificial and depends on the summed area. Only the suppression around the Fermi energy is essential.

There exists a gap structure also in the density of states. However, because of the peak due to the quasiparticles around $(\pi/2, \pi/2)$, the gap structure of the density of states is not so clear as that in the superconducting states, or that of the spectral weight in the vicinity of $(0, \pi)$. These results are consistent with the tunneling spectroscopy experiments.¹²⁾

Thus, most of the features related to the pseudogap phenomena are understood from the above

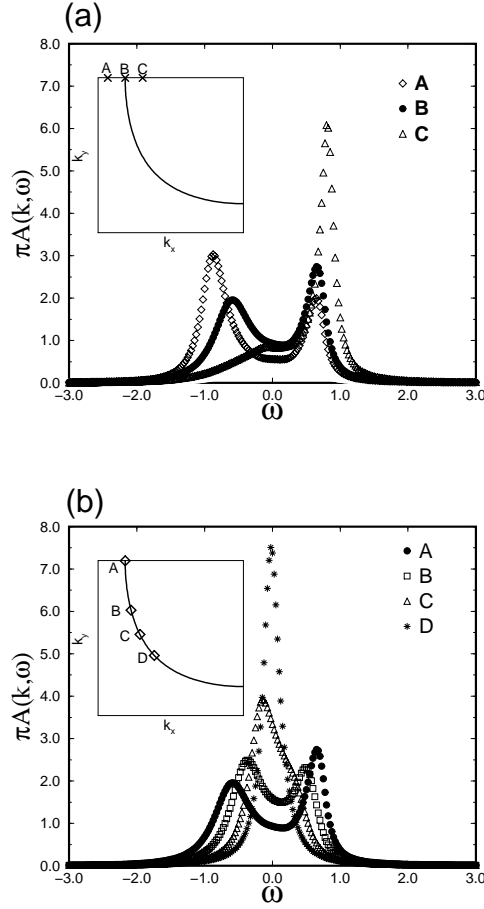


Fig. 10. The momentum dependence of the spectral weight (a) across the Fermi surface near $(0, \pi)$ (b) along the Fermi surface. The respective k -points are shown in the inset. The other parameters are the same as those in Fig. 8.

lowest order calculation. From the above results, we conclude at least that the strong coupling superconductivity makes the Fermi liquid state unstable near the mean field superconducting critical temperature T_{MF} .

As we have pointed out before, the above calculation is applicable to the higher temperature than T_{MF} . In practice, the effects of the superconducting fluctuations remarkably suppress the critical temperature. Indeed, we have an interest in the temperature region in which the superconductivity is suppressed by the fluctuations. In order to treat this region explicitly, we must carry out the self-consistent calculation using the renormalized Green function. We will carry out the self-consistent

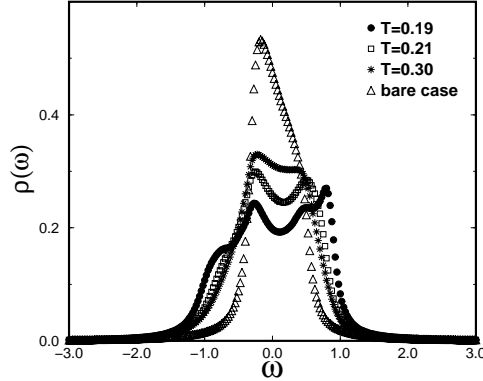


Fig. 11. The density of states $\rho(\varepsilon)$ for various temperatures. The parameters and the marks are the same as those in Fig.8. The triangles show the non-interacting density of states. Since we calculate only in the vicinity of the Fermi surface, the peak position is not exact. The suppression of the density of states at the low energy is essential.

calculation in the next section, §4. Although there are some differences, the essential results, such as the gap structure and so on, do not change even in the self-consistent calculation.

§4. Self-Consistent Calculation

In this section, we self-consistently calculate the single particle self-energy and the TDGL parameters on the basis of the formalism described in §2. Furthermore, we calculate the superconducting critical temperature suppressed by the effects of the fluctuations, and determine the phase diagram.

To begin with, we explain our method of the numerical calculation used in this section. We restrict the \mathbf{k} - points for which the self-energies are calculated to the region close to the Fermi surface. The restricted region is shown in Fig.12. As we have mentioned in the previous section, the effects of the superconducting fluctuations (resonances) are important in the vicinity of the Fermi surface, and are not important far from the Fermi surface. Except for a_1 , the TDGL parameters mainly depends on the electron states near the Fermi surface. Furthermore, the important \mathbf{k} -points for the self-consistent calculation of the self-energy $\Sigma^R(\mathbf{k}, \omega)$ exist only in the vicinity of \mathbf{k} , because the main contribution is given by the terms with the momentum in the vicinity of $\mathbf{q} = 0$. Therefore, we have only to consider the self-energy near the Fermi surface. Thus, our restriction for the momentum space is justified.

We estimate the TDGL parameters by eq. 2.6 for the renormalized Green function $G^R(\mathbf{k}, \omega) =$

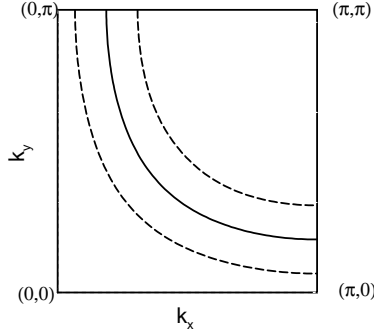


Fig. 12. In this section, the self-energy is calculated in the region between the dashed lines.

$(\omega - \varepsilon_{\mathbf{k}} - \Sigma^{\text{R}}(\mathbf{k}, \omega))^{-1}$, and self-consistently calculate the single particle self-energy $\Sigma^{\text{R}}(\mathbf{k}, \omega)$, using eq. 2.13 (see Fig.5(b)). Here, we exclude the Hartree-Fock term corresponding to the diagram in Fig.4(c), as we have done in the lowest order calculation in §3. This calculation corresponds to the self-consistent T-matrix approximation (see Fig.4(b)).

For the purpose of the self-consistent calculation, we divide the Brillouin zone as shown in Fig.12, and put $\Sigma^{\text{R}}(\mathbf{k}, \omega) = 0$ outside of the dashed lines. As we have described before, this approximation does not change the structure near the Fermi surface and is appropriate to discuss the pseudogap phenomena.

Furthermore, we introduce the cutoff parameters for the integrations by Ω and \mathbf{q} , because the main contribution is obtained from the integrations around $\mathbf{q} = \Omega = 0$. Owing to the cutoff, we might slightly underestimate the effects of the superconducting fluctuations. However, the cutoff procedure has no significant effect on our results. Moreover, the TDGL expansion is not so reliable for large \mathbf{q} and Ω .

It should be noticed that in this self-consistent calculation we fix the parameter t_0 instead of the coupling constant g . Although the final self-consistent results are identical, the convergence of the solution is remarkably improved by using this method. In particular, we need to adopt this method in order to calculate near the superconducting critical point where the superconducting fluctuations are strong. The parameter t_0 represents the distance from the superconducting critical point. Therefore, if the parameter t_0 is varied, the situation remarkably changes. As a result, the solution fluctuates for the g -fixed calculations in many cases.

Thus, because of the convenience of the numerical calculation, not the coupling constant g but the temperature T and the parameter t_0 are fixed in our calculation. The coupling constant g is a

quantity determined by a result of the self-consistent calculation.

We do not positively change the chemical potential so as to conserve the particle number. However, we have verified that the particle number is almost conserved in this calculation.

Strictly speaking, the superconducting transition does not occur in the two-dimensional systems. The fact is known as the Marmin-Wagner's theorem. As we have described in §2, our calculations also reflect the fact. The superconducting critical temperature $T_c = 0$ in our formalism because of the logarithmic singularity of the self-energy due to the two-dimensional singularity. However, the weak three-dimensionality is sure to remove these singularities in the realistic layered systems.³⁹⁾ Therefore, we phenomenologically introduce the three-dimensionality and define the superconducting critical temperature as the temperature in which $1 + g\chi_0(\mathbf{0}, 0) = 0.01$. This condition corresponds to the 100 times enhancement of the superconducting susceptibility. The phase diagram does not depend on the details of this definition, qualitatively.

We show the results of the spectral weight for various t_0 and temperatures in Fig.13.

The gap structure exists in the small t_0 cases, and becomes clear as t_0 decreases. Then, the properties of the TDGL parameters reproduce our argument in §2. That is to say, the superconducting fluctuations are propagative and have the small dispersion. Because the parameter t_0 shows the closeness to the superconducting critical point, these behaviors are natural. The effects of the resonances are rather drastic in case of the high temperature, that is to say, large $|g|$, where the thermal fluctuations are rather strong.

In particular, the plural peak structure appears in the small t_0 and large T cases. This complicated structure is also understood on the basis of the resonance formalism as we explain below. For example, we show the self-energy for $T = 0.10$, $t_0 = 0.01$ in Fig.14. In this case, the spectral weight has three peak structure.

It should be noticed that the electronic structure around $(-\mathbf{k}, -\omega)$ plays an important role for the estimate of the self-energy $\Sigma^R(\mathbf{k}, \omega)$. It is because the main contribution comes from the integrations in the vicinity of $\mathbf{q} = \Omega = 0$. Therefore, if the spectral weight has its peak at $\omega = \omega_p$, the real part of the self-energy has the positive slope at $\omega = -\omega_p$, and the imaginary part has the peak at $\omega = -\omega_p$ in its absolute value. In rough estimate, $\text{Im}\Sigma^R(\mathbf{k}, \omega) \propto A(\mathbf{k}, -\omega)$.

To put it in detail, the left peak and the middle peak yield the positive slope of the real part on the positive frequency side, and yield the right peak. The right peak yields the positive slope of the real part on the negative frequency side. Consequently the negative slope is formed at the small negative frequency. The only solution $\omega - \varepsilon_{\mathbf{k}} - \text{Re}\Sigma^R(\mathbf{k}, \omega) = 0$ exists here. It corresponds to the middle peak. Moreover, the right peak yields the sharp peak of $-\text{Im}\Sigma^R(\mathbf{k}, \omega)$ at the negative frequency side. The peak yields the double peak structure on the negative frequency side. They

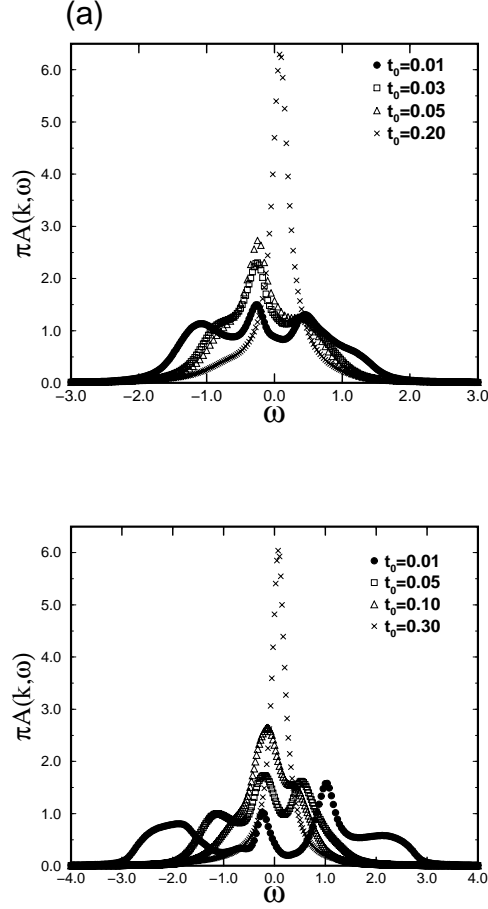


Fig. 13. The spectral weight on the Fermi surface near $(0, \pi)$ obtained by the self-consistent calculation. (a) $T = 0.10$. t_0 is varied as 0.01, 0.03, 0.05, 0.20. (b) $T = 0.15$. t_0 is varied as 0.01, 0.05, 0.10, 0.30. The calculated points are shown in the phase diagram (Fig.17). The \mathbf{k} -point is the same as that in Fig.8.

correspond to the left and middle peaks. It should be noticed that such an asymmetric structure stabilizes the self-consistent solution. Because of the rough relation $\text{Im}\Sigma^{\text{R}}(\mathbf{k}, \omega) \propto A(\mathbf{k}, -\omega)$, the peak of the spectral weight at ω_p will extinguish the peak at $-\omega_p$. In particular, the spectral weight at the Fermi energy $\omega = 0$ is necessarily suppressed. Thus, the symmetric structure is unstable in our formalism. Therefore, the gap formation is difficult in the particle-hole symmetric models, although it is not impossible in the strong coupling case.

As we mentioned in §2, the particle-hole asymmetry naturally exists in the real systems and the asymmetry is essential for the self-consistent solution to be stabilized. Furthermore, High- T_c

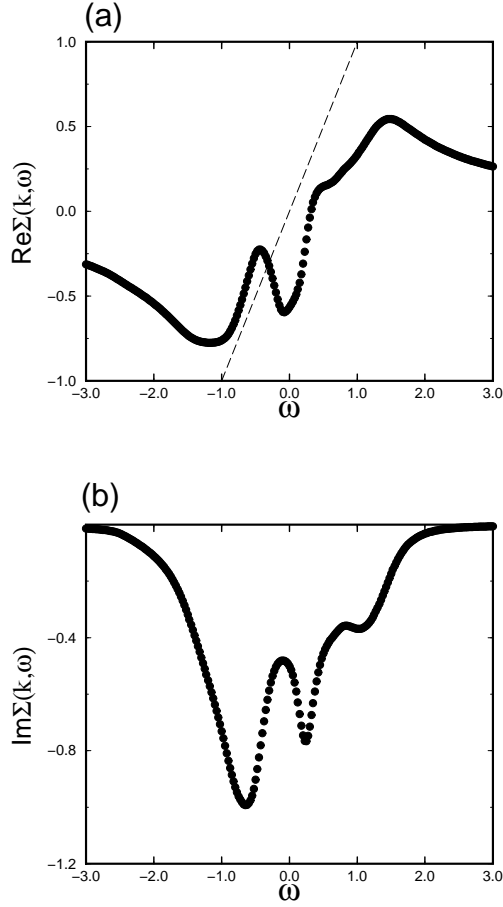


Fig. 14. The single particle self-energy on the Fermi surface near $(0, \pi)$. Here, $T = 0.10$, $t_0 = 0.01$. (a)The real part. The long-dashed line is described in order to show the line $\omega - \varepsilon_{\mathbf{k}} - \text{Re}\Sigma^{\text{R}}(\mathbf{k}, \omega) = 0$. (b)The imaginary part. The \mathbf{k} -point is the same as that in Fig.8.

cuprates are the strongly asymmetric systems because of existence of the Van-Hove singularity.

It is notable that these results are not consistent with the assumption by Norman *et al.*⁴⁶⁾ and Maly *et al.*³²⁾ Although the rough features of their phenomenological self-energy remain in our explicit self-consistent calculation, their assumption cannot satisfy the self-consistency.

Here, we pay attention to the change of the spectral weight, once more. In the phase diagram (Fig.17), we show the parameters for which we show the spectral weight or the density of states.

When t_0 is large and the temperature T is higher than the mean field critical temperature T_{MF} , the spectral weight has the sharp single peak structure. This structure is of the conventional Fermi

liquid theory.

As t_0 decreases and the temperature becomes lower than T_{MF} , the peak shifts to the negative frequency side and has the long tail to the positive frequency side. In this region, as the momentum is varied from $(0, \pi)$ to (π, π) , the peak shifts to positive frequency side and cross the Fermi level $\omega = 0$. However, as a result of resonances, the damping rate $-\text{Im}\Sigma^R(\mathbf{k}, \omega)$ is large at the Fermi level and the spectral weight is suppressed there. Therefore, the density of states is reduced at the Fermi level. The superconducting fluctuations gradually become propagative.

As t_0 decreases further and the system approaches to the critical point, the spectral weight has the plural peak structure. This behavior is quite different from that of the conventional Fermi liquid theory.

Here, we show the density of states for $T = 0.10$ and various t_0 in Fig.15.

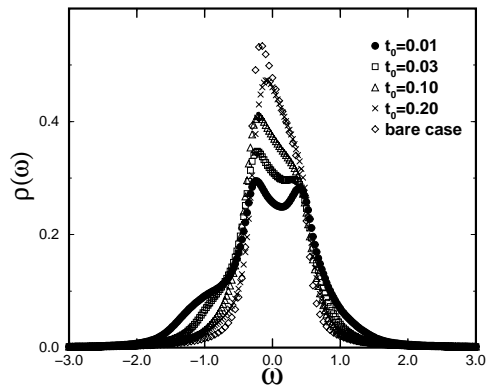


Fig. 15. The density of states $\rho(\omega)$ for $T = 0.10$. t_0 is varied as 0.01, 0.03, 0.10, 0.20. The diamonds show the non-interacting density of states. Since we calculate only the states in the vicinity of the Fermi surface, the peak position is not exact. The suppression of the density of states at the low energy is essential.

As we mentioned above, the density of states at the Fermi level is reduced as a result of the resonance effects. In particular, in case of $t_0 = 0.10$, the spectral weight has a sharp single peak in the vicinity of the Fermi surface. However, we can see clearly the suppression of the density of states. Generally speaking, the suppression becomes distinguished at the mean field critical temperature T_{MF} . The suppression becomes more remarkable, as t_0 decreases and the system approaches the critical point. In the vicinity of the critical point, the density of states at the Fermi

level is mainly given by the contribution from the quasiparticles near $(\pi/2, \pi/2)$. Therefore, $\rho_d(0)$ is more remarkably reduced by the effects of the resonances.

Here, we show the momentum dependence of the spectral weight for the typical three peak case in Fig.16.

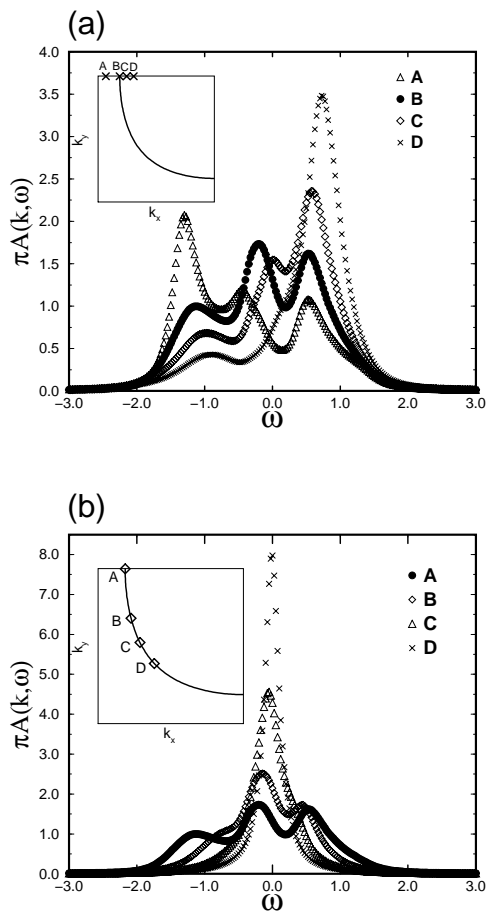


Fig. 16. The momentum dependence of the spectral weight. Here, $T = 0.15$, $t_0 = 0.05$. The momentum is varied (a) across the Fermi surface near $(0, \pi)$ (b) along the Fermi surface. The respective k -points are shown in the inset.

In Fig.16(a), the momentum is varied across the Fermi surface near $(0, \pi)$. On the negative energy side from the Fermi surface, the spectral weight transfers to the left peak. On the other hand, it transfers to the right peak on the opposite side from the Fermi surface. All peaks shift to the positive frequency side with the momentum shift. It should be noticed that the middle

peak shifts and is found at the Fermi level $\omega = 0$ when the momentum slightly deviates from the Fermi surface (represented as C in the inset). However, it is strongly reduced by the effects of the fluctuations. With increasing k_x , this peak cannot cross the Fermi level $\omega = 0$ and disappears at last. Thus, the spectral weight shows the double peak structure at D (see the inset).

In Fig.16(b), the momentum is varied along the Fermi surface. We can see that the gap structure is remarkable in the vicinity of $(0, \pi)$ where the attractive interaction is strong, and becomes inconspicuous as the momentum approaches to $(\pi/2, \pi/2)$. Furthermore, the single peak of quasi-particles exists in the vicinity of $(\pi/2, \pi/2)$. This fact shows that the Fermi liquid like behavior exists in this region. Thus, it is naturally led from our formalism that the pseudogap has the same shape as the superconducting gap, as suggested by the ARPES experiments.¹¹⁾

Last of all, we show the phase diagram in Fig.17. We show the mean field critical temperature T_{MF} and the actual critical temperature T_c calculated self-consistently.

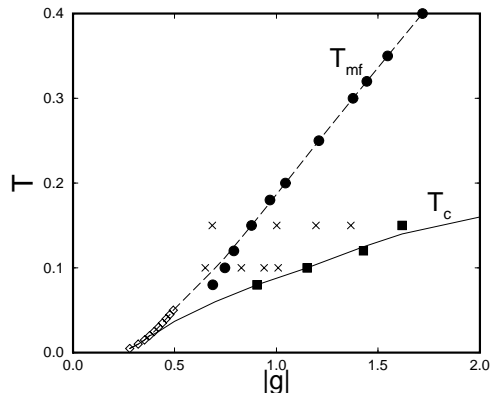


Fig. 17. The phase diagram obtained in this paper. The circles and diamonds show the superconducting critical temperature based on the mean field theory (T_{MF}). The circles are obtained by using the discrete momentum used in our self-consistent calculation. The diamonds are obtained by the explicit calculation for eq. 2.8. The circles at the low temperature are slightly off by the numerical error. The squares show the actual superconducting critical temperature (T_c) suppressed by the fluctuations. The suppression becomes stronger in the strong coupling region. The marks \times show the points where we have shown the spectral weight or the density of states. They correspond to $t_0 = 0.20, t_0 = 0.10, t_0 = 0.05, t_0 = 0.03$ from left to right for $T = 0.10$, and $t_0 = 0.30, t_0 = 0.10, t_0 = 0.05, t_0 = 0.03$ for $T = 0.15$, respectively. As we mentioned in this article, the squares correspond to $t_0 = 0.01$.

The superconducting critical temperature (T_c) is strongly reduced by the fluctuations. This effect

is mainly caused by the suppression of the density of states. As the coupling constant increases, the reduction of the critical temperature becomes remarkable. It should be noticed that this effect is different from that of the Nozières and Schmitt-Rink formalism. According to the Nozières and Schmitt-Rink formalism, the critical temperature is reduced by the shift of the chemical potential. The chemical potential shifts so that the density of state decreases. In our formalism, the density of states is reduced by the effects of the resonances with the thermally excited weakly-damped pre-formed pairs.

Roughly speaking, the pseudo-gap phenomena occurs in the region between T_{MF} and T_c . This region is extremely wide in the strong coupling case.

The density of states starts to decrease, roughly at T_{MF} . Most of the physical quantities measured by the various experiments, such as NMR,^{2,3)} optical conductivity,⁴⁾ tunneling spectroscopy¹²⁾ and so on, reflect the density of state. Therefore, their experiments should show some changes at T_{MF} . Actually, various changes around T_{MF} are reported by several experiments.⁶⁾

Moreover, the ARPES experiments directly reflect the spectral weight. In our calculation, the quasiparticle's peak starts to shift to the negative frequency side and become broad at T_{MF} . As the temperature approaches to T_c , the spectral weight at $\omega = 0$ is strongly reduced. This reduction of the spectral weight has been observed by the ARPES experiments.¹¹⁾ The plural peak structure of the spectral weight is also observed by the ARPES experiments.⁴⁸⁾ However, since the spectral weight is extremely broad when the plural peak structure appears, such a structure may not be observed actually. Moreover, by summing up the momentum around the measured momentum, corresponding to the experimental resolving power, the plural peak structure may disappear. The reduction of the spectral weight at the Fermi energy $\omega = 0$ is essential. In this sense, our calculation is consistent with the ARPES experiments.

On the other hand, the specific heat starts to decrease at rather higher temperature.¹⁵⁾ We think that in the strongly correlated electron systems, the entropy mainly originates from the freedom of spins. Therefore, the specific heat is expected to be sensitive to the anti-ferromagnetic spin fluctuations. The anti-ferromagnetic correlation exists at rather higher temperature than T_{MF} in high- T_c cuprates. Although we do not take account of its effects in this paper, we consider that the specific heat is reduced by the anti-ferromagnetic spin fluctuations. The recent experiment⁴⁹⁾ shows that the specific heat decreases still more, but only slightly at T_{MF} . This fact is naturally explained by our calculation in this paper which shows the suppression of the density of states.

§5. Summary and Discussion

In this paper, we have calculated the effects of the strong coupling superconductivity on the normal state electronic structure. We have considered that the strong coupling superconductivity takes place in under-doped High- T_c cuprates and the pseudogap phenomena are its precursor.

We took account of the realistic situation, such as the two-dimensionality, the d -wave symmetry

of the pairs, the lattice system near the half-filling, the particle-hole asymmetry and so on.

First, we considered the T-matrix which is the dominant scattering vertex in the vicinity of the superconducting critical point. Since the T-matrix diverges at $\mathbf{q} = \Omega = 0$ at the critical point (Thouless criterion), we expand the reciprocal of the T-matrix with respect to \mathbf{q}^2 and Ω (TDGL expansion) and study its contribution to the single particle self-energy from the small \mathbf{q} and Ω region.

We showed that although the superconducting fluctuations are strongly diffusive in the weak coupling limit, they are propagative and possess the character as the pre-formed pairs in case of the strong coupling superconductivity. In particular, the pre-formed pairs have the hole-like character reflecting the band structure of High- T_c cuprates.

On the basis of the above argument, we analytically calculated the self-energy and showed the anomalous behaviors of the self-energy, using the phenomenologically introduced TDGL parameters. In particular, the real part of the self-energy has the large positive slope near $\alpha = \omega + \varepsilon_{\mathbf{k}} = 0$, and the imaginary part has the sharp peak in its absolute value there. These features are quite different from those given by the conventional Fermi liquid theory. Such a self-energy leads to the gap-like structure of the spectral weight. Furthermore, because of the hole-like character of the pre-formed pairs, the asymmetric structure is naturally introduced. The peak of the spectral weight is relatively broad on the negative frequency side, and sharp on the positive frequency side. These are the effects of the resonances of quasiparticles with the thermally excited weakly-damped pre-formed pairs.

Furthermore, we explicitly estimated the TDGL parameters and calculated the self-energy for the bare Green function $G^{\text{R}(0)}(\mathbf{k}, \omega)$, and the renormalized Green function $G^{\text{R}}(\mathbf{k}, \omega)$ which we refer to the lowest order calculation and the self-consistent calculation, respectively. They correspond to the T-matrix approximation and the self-consistent T-matrix approximation, respectively.

In the lowest order calculation, since the damping rate of the pre-formed pairs is not suppressed by the renormalization, the effects of the resonances are smaller than those obtained by our analytic calculation. However, the self-energy has the same features as those of our analytic calculation. As a result, the spectral weight shows the gap-like structure.

By carrying out the self-consistent calculation, we confirmed the change of the TDGL parameters by the renormalization effects which we argued in §2. Furthermore, the self-energy has the relevant features to the idea of the resonances. They are not consistent with the assumption by Norman *et al.*⁴⁶⁾ and Maly *et al.*³²⁾ However, the spectral weight necessarily shows the gap-like structure in the vicinity of the superconducting critical point, although the structure is quite different from that assumed by Norman *et al.*⁴⁶⁾ and Maly *et al.*³²⁾ The structure is extremely asymmetric and the spectral weight is strongly reduced at the Fermi level. This asymmetry, which is essential for the idea of the resonances, stabilizes the self-consistent solution. Since the asymmetric structure

is neglected in the assumption by Norman *et al.*⁴⁶⁾ and Maly *et al.*,³²⁾ their assumption cannot satisfy the self-consistency. By summing up the momentum, we obtained the density of states in which the complicated structure disappears. As a result, the density of states is also suppressed at the Fermi level by the effects of the resonances.

The effects of the superconducting fluctuations manifest at the mean field superconducting critical temperature T_{MF} . The density of states starts to decrease at T_{MF} and the characteristic change appears in the various quantities. These are the pseudogap phenomena and are consistent with experiments.⁶⁾

We obtained the phase diagram by the self-consistent calculation. The superconducting critical temperature T_c is reduced by the suppression of the density of states. The reduction becomes more remarkable as the coupling constant increases. Therefore, although the mean field critical temperature T_{MF} remarkably increases with the coupling constant $|g|$, T_c does not vary so much. The pseudogap phenomena take place between T_{MF} and T_c . Therefore, the pseudogap exists in the wide region in the strong coupling case.

Considering that the band width ε_F is renormalized by the electron-electron correlation, the ratio T_c/ε_F is increased by the renormalization. As the doping quantity decreases, the system approaches to the Mott insulator. Therefore, it is natural to consider that the renormalization effects are enhanced with decreasing doping quantity. Since the anti-ferromagnetic spin fluctuations are enhanced at the same time, the attractive interaction becomes strong in the under-doped region. Therefore, it is natural to consider that the superconductivity effectively becomes the strong coupling, with decreasing doping quantity.

Both T_c and T_{MF} are scaled by the band width ε_F . By considering these facts, it is naturally understood that T_c decreases with the doping rate, although T^* doesn't so. Since T_c/ε_F is almost independent of the coupling constant $|g|$ in the strong coupling region, T_c decreases with ε_F in the under-doped region. On the other hand, $T_{\text{MF}}/\varepsilon_F$ increases with $|g|$. Therefore, T_{MF} increases with the attractive interaction $|g|$ in spite the decrease of the effective band width ε_F in the under-doped region.

Thus, our theory naturally and appropriately explains the pseudogap phenomena in High- T_c cuprates.

Of course, the anti-ferromagnetic spin fluctuations are important to explain some experiments. In particular, they play a dominant role in the temperature region higher than T^* . For example, the NMR spin lattice relaxation rate $1/T_1$ is enhanced at the higher temperature than T^* and the electronic specific heat is reduced well above T^* . We consider that these behaviors are attributed to the effects of the anti-ferromagnetic spin fluctuations. We do not take account of the effects. However, the so-called pseudogap phenomena which are experimentally observed bellow T^* are naturally understood as the precursor of the d -wave strong coupling superconductivity.

Here, we mention some important factors in our theory. Of course, the strong coupling superconductivity is most essential. The coupling constant g does not appear explicitly. However, it is included in the properties of the TDGL parameters. In particular, it is essential that b and a_2 are reduced in the strong coupling case by the renormalization. The lattice system near the half-filling is important for the resonance effects. The effects of the resonances are different from that of Nozières and Schmitt-Rink formalism which is justified in the low density limit. The two-dimensionality is essential because it leads to the strong fluctuations which are characteristics of the low-dimensional systems. The particle-hole asymmetry is also important to stabilize the self-consistent solution.

These factors properly reflect the characteristics of High- T_c cuprates. Thus, the realistic treatment carried out in this paper is necessary for the pseudogap phenomena. In other words, the pseudogap phenomena well represent the individuality of High- T_c cuprates.

Here, it should be noted that although we have emphasized the importance of the particle-hole asymmetry, the pseudogap formation is possible in principle even in the particle-hole symmetric case. (Actually, this is a perfect nesting case and is not realistic.) In the symmetric case $a_1 = 0$, and the superconducting fluctuations are diffusive. However, it is the same that the small \mathbf{q} and Ω region make a dominant contribution for the self-energy. Therefore, the strong fluctuations necessarily make the Fermi liquid state unstable even in the symmetric models. After all, the pseudogap formation is relatively difficult but not impossible in the symmetric case.

Here, we give a discussion on the magnetic scenarios for the pseudogap phenomena. The calculation treating the pseudogap phenomena as a precursor of the magnetic instability (anti-ferromagnetism or SDW) has been calculated.¹⁸⁾ We also think it should be possible that the strong spin fluctuations near the magnetic critical point lead to the gap-like structure. In that case, the gap formation first takes place at 'hot spot', because the interaction is strong in the vicinity of $\mathbf{q} = (\pi, \pi)$ and $\Omega = 0$. Since the spin fluctuations lead to the transformation of the Fermi surface, 'hot spot' comes to exist in the wide region near $(0, \pi)$.⁹⁾ Therefore, the gap structure would have a similar shape to the $d_{x^2-y^2}$ -wave superconducting gap.

However, we think it does not occur in High- T_c cuprates. Since the interaction caused by the superconducting fluctuations is strong in the vicinity of $\mathbf{q} = (0, 0)$, the important \mathbf{k} -points for the self-energy on the Fermi surface are sure to be on the Fermi surface. On the other hand, in case of the anti-ferromagnetic spin fluctuations, the interaction is strong in the vicinity of $\mathbf{Q} = (\pi, \pi)$. Therefore, the important \mathbf{k} -points for the quasiparticles with the momentum \mathbf{k} exist in the vicinity of $\mathbf{k} + \mathbf{Q}$. They are on the Fermi surface only when \mathbf{k} is on the 'hot spot'.⁹⁾ As a result, the quasiparticles slightly apart from 'hot spot' are not directly scattered by the strong interaction. Thus, the pseudogap formation is not impossible but difficult to be attributed to the magnetic interaction on the numerical point of view. Moreover, since the phase transition which really occurs is the superconductivity, the superconducting critical phenomena necessarily take place.

It is not obvious how the critical spin fluctuations can exist even in the critical region of the superconductivity. Indeed, the spin fluctuations have turned out to be reduced in the pseudogap region. Furthermore, the continuity at the superconducting critical point is difficult to be explained naturally by the magnetic scenarios.

On the other hand, a slight suppression of the density of states is indicated at the rather higher temperature than T^* .¹²⁾ We expect that it is derived from the effects of the anti-ferromagnetic spin fluctuations.

Here, we shortly discuss the magnetic field dependence of the pseudogap phenomena. A recent experiment by Gorny *et al.*⁵⁰⁾ has reported that the NMR spin lattice relaxation rate $1/T_1$ has no magnetic field dependence around the pseudogap onset temperature T^* . On the other hand, Mitrović *et al.* have reported that $1/T_1$ has the magnetic field dependence⁵¹⁾ and given the comment that their sample is optimally-doped and that of Gorny *et al.* is under-doped.⁵²⁾ Because the pseudogap phenomena continuously take place from optimally-doped to under-doped cuprates, these magnetic field dependences also should be understood continuously.

The pseudogap effects are expected to be relatively small in optimally-doped cuprates. Eschrig *et al.* have shown that the magnetic field dependence of the optimally-doped cuprates is consistent with the results of the conventional d -wave superconducting fluctuation theory.⁴²⁾ In their calculation, the DOS corrections play an important role. As we mentioned in the previous sections, our theory is a natural extension of their conventional approach.

As the coupling constant $|g|$ increases, the characteristic length $\xi \propto b^{\frac{1}{2}}$ of the orbital motion of the pre-formed pairs decreases. Generally speaking, the main effect of the magnetic field is the Landau quantization. Owing to the Landau quantization, \mathbf{q}^2 is quantized. The coefficient of \mathbf{q}^2 is $b \propto \xi^2$ and is small in the strong coupling case. Moreover, t_0 is relatively large near the onset temperature T^* . Since the effects of the magnetic fields are actually scaled by b/t_0 , the effects are further small near T^* . Therefore, we think that the magnetic field dependence is relatively weak in the strong coupling case, that is, in under-doped cuprates. The fact is especially concluded near T^* . Thus, the pairing scenario for the pseudogap phenomena discussed in this paper does not contradict with the continuous comprehension of the magnetic field dependences.

The continuity of the phase diagram of High- T_c cuprates are understood as described below on the basis of our scenario. As the doping rate decreases from the over-doped region, the band width ε_F is renormalized and the critical temperature T_c increases. Then, T_c/ε_F gradually increases, and the effects of the superconducting fluctuations appear. When the doping rate decreases further and cross the optimally-doped region, the strong coupling superconductivity described in this paper is realized and the pseudogap phenomena occur in the wide temperature region.

The definite calculations for the physical quantities such as the spin lattice relaxation rate, the spin susceptibility, the specific heat, the transport coefficients and so on are the important future

problems.

As we have mentioned above, the strong coupling superconductivity takes place in the electron systems renormalized by the strong repulsive interaction. The formulation of the strong coupling superconductivity for the strongly renormalized quasiparticles is a greatly important future problem.

Acknowledgements

The authors are grateful to Professor M. Ido, Professor M. Oda and Dr. N. Momono for fruitful discussions, and to Professor T. Takahashi for valuable comments. Numerical computation in this work was partly carried out at the Yukawa Institute Computer Facility. The present work was partly supported by a Grant-In-Aid for Scientific Research from the Ministry of Education, Science, Sports and Culture, Japan. One of the authors (Y.Y) has been supported by a Research Fellowships of the Japan Society for the Promotion of Science for Young Scientists.

-
- 1) J. G. Bednortz and K. A. Müller: *Z. Phys. B* **64** (1986) 189.
 - 2) W. W. Warren, R. E. Walstedt, G. F. Brennert, R. J. Cava, R. Tycko, R. F. Bell and G. Dabbagh: *Phys. Rev. Lett.* **62** (1989) 1193.; M. Takigawa, A. P. Reyes, P. C. Hammel, J. D. Thompson, R. H. Heffner, Z. Fisk and K. C. Ott: *Phys. Rev. B* **43** (1991) 247.; M. H. Julien, P. Carretta, M. Horvatić: *Phys. Rev. Lett.* **76** (1996) 4238.; H. Yasuoka, S. Kambe, Y. Itoh and T. Machi: *Physica. B* **199&200** (1994) 278.; Y. Itoh, T. Machi, S. Adachi, A. Fukuoka, K. Tanabe and H. Yasuoka: *J. Phys. Soc. Jpn.* **67** (1998) 312.;
 - 3) K. Ishida, K. Yoshida, T. Mito, Y. Tokunaga, Y. Kitaoka, K. Asayama, Y. Nakayama, J. Shimoyama and K. Kishio: *Phys. Rev. B* **58** (1998) R5960.
 - 4) C. C. Homes, T. Timusk, R. Liang, D. A. Bonn and W. H. Hardy : *Phys. Rev. Lett.* **71** (1993) 1645.
 - 5) For example, T. Ito, K. Takenaka and S. Uchida: *Phys. Rev. Lett.* **70** (1993) 3995.; K. Mizuhashi, K. Takenaka, Y. Fukuzumi and S. Uchida: *Phys. Rev. B* **52** (1995) R3884.
 - 6) M. Oda, K. Hoya, R. Kubota, C. Manabe, N. Momono, T. Nakano and M. Ido: *Physica. C* **281** (1997) 135.
 - 7) For example, K. Takenaka, K. Mizuhashi, H. Takagi and S. Uchida: *Phys. Rev. B* **50** (1994) 6534.; Y. Nakamura and S. Uchida: *Phys. Rev. B* **47** (1993) 8369.
 - 8) B. P. Stojković and D. Pines: *Phys. Rev. Lett.* **76** (1996) 811.; B. P. Stojković and D. Pines: *Phys. Rev. B* **55** (1997) 8576.
 - 9) Y. Yanase and K. Yamada: *J. Phys. Soc. Jpn* **68** (1999) 548.
 - 10) H. Ding, T. Yokoya, J. C. Campuzano, T. Takahashi, M. Randeria, M. R. Norman, T. Mochiku, K. Kadowaki and J. Giapintzakis: *Nature*. **382** (1996) 51.; A. G. Loeser, Z. X. Shen, D. S. Dessau, D. S. Marshall, C. H. Park, P. Fournier and A. Kapitulnik: *Science*. **273** 325.
 - 11) M. R. Norman, H. Ding, M. Randeria, J. C. Campuzano, T. Yokoya, T. Takeuchi, T. Takahashi, T. Mochiku, K. Kadowaki, P. Guptasarma and D. G. Hinks: *Nature*. **392** (1998) 157.
 - 12) Ch. Renner, B. Revaz, J.-Y. Genoud, K. Kadowaki and Ø. Fischer: *Phys. Rev. Lett.* **80** (1998) 149.
 - 13) Ch. Renner, B. Revaz, K. Kadowaki, I. Maggio-Aprile and Ø. Fischer: *Phys. Rev. Lett.* **80** (1998) 3606.
 - 14) J. L. Tallon, C. Bernhard, G. V. M. Williams and J. W. Loram: *Phys. Rev. Lett.* **79** (1997) 5294.
 - 15) J. W. Loram, K. A. Mirza, J. M. Wade, J. R. Cooper and W. Y. Liang: *Physica. C* **235-240** (1994) 134.
 - 16) T. Tanamoto, H. Kohno and H. Fukuyama: *J. Phys. Soc. Jpn* **63** (1994) 2739.

- 17) A. Kampf and J. R. Schrieffer: Phys. Rev. B **41** (1990) 6399.; A. V. Chubukov, D. K. Morr and K. A. Shakhnovich: Philos. Mag. B **74** (1996) 563.; D. Pines: Z. Phys. B **103** (1997) 129.
- 18) T. Dahm and L. Tewordt: Phys. Rev. B **52** (1995) 1297.
- 19) P. Nozières and S. Schmitt-Rink: J. Low Temp. Phys. **59** (1985) 195.
- 20) A. J. Leggett: *Modern Trends in the Theory of Condensed Matter* ed. A. Pekalski and R. Przystawa (Springer-Verlag, Berlin, 1980).
- 21) S. Schmitt-Rink, C. M. Varma and A. E. Ruckenstein: Phys. Rev. Lett. **63** (1989) 445.
- 22) A. Tokumitsu, K. Miyake and K. Yamada: Prog. Theor. Phys. Suppl. **106** (1991) 63.
- 23) M. Randeria: preprint. (cond-mat/9710223); C. A. R. Sá de Melo, M. Randeria and J. R. Engelbrecht: Phys. Rev. Lett. **71** (1993) 3202.
- 24) S. Stintzing and W. Zwerger: Phys. Rev. B **56** (1997) 9004.
- 25) R. Haussmann: Phys. Rev. B **49** (1994) 12975.
- 26) S. Koikegami and K. Yamada: J. Phys. Soc. Jpn. **67** (1998) 1114.
- 27) V. J. Emery and S. A. Kivelson: Phys. Rev. Lett. **74** (1995) 3253.
- 28) H. J. Kwon and A. T. Dorsey: Phys. Rev. B **59** (1999) 6438.
- 29) V. B. Geshkenbein, L. B. Ioffe and A. I. Larkin: Phys. Rev. B **55** (1997) 3173.
- 30) J. R. Engelbrecht, A. Nazarenko, M. Randeria and E. Dagotto: Phys. Rev. B **57** (1998) 13406.
- 31) T. Ichinomiya and K. Yamada: J. Phys. Soc. Jpn. **68** (1999) 981.
- 32) J. Maly, B. Jankó and K. Levin: preprint. (cond-mat/9805018); Q. Chen, I. Kosztin, B. Jankó and K. Levin: Phys. Rev. B **59** (1999) 7083.
- 33) T. Dahm, D. Manske and L. Tewordt: Phys. Rev. B **55** (1997) 15274.
- 34) S. Koikegami and K. Yamada: private communication.
- 35) L. G. Aslamazov and A. I. Larkin: Fiz. Tverd. Tela. **10** (1968) 1104. [Sov. Phys. Solid State **10** (1968) 875.]
- 36) K. Maki: Prog. Theor. Phys **40** (1968) 193.; R. S. Thompson: Phys. Rev. B **1** (1970) 327.
- 37) K. Kuboki and H. Fukuyama: J. Phys. Soc. Jpn **58** (1989) 376.
- 38) J. Heym: J. Low Temp. Phys. **89** (1992) 869.
- 39) M. Randeria and A. A. Varlamov: Phys. Rev. B **50** (1994) 10401.
- 40) C. Di Castro, R. Raimondi, C. Castellani and A. A. Varlamov: Phys. Rev. B **42** (1990) 10221.
- 41) A. A. Varlamov, G. Balestrino, E. Milani and D. V. Livanov: preprint. (cond-mat/9710175v2)
- 42) M. Eschrig, D. Rainer and J. A. Sauls: Phys. Rev. B **59** (1999) 12095.
- 43) H. Ebisawa and H. Fukuyama: Prog. Theor. Phys **46** (1971) 1042.
- 44) H. Fukuyama, H. Ebisawa and T. Tsuzuki: Prog. Theor. Phys **46** (1971) 1028.
- 45) A. G. Aronov and A. B. Rapoport: Mod. Phys. Lett. B **6** (1992) 1083.
- 46) M. R. Norman, M. Randeria, H. Ding and J. C. Campuzano: Phys. Rev. B **57** (1998) 11093.
- 47) M. Randeria, H. Ding, J. C. Campuzano, A. Bellman, G. Jennings, T. Yokoya, T. Takahashi, H. Katayama-Yoshida, T. Mochiku and K. Kadowaki: Phys. Rev. Lett. **74** (1995) 4951.
- 48) T. Takahashi: private communication.
- 49) M. Ido, M. Oda and N. Momono: private communication.
- 50) K. Gorny, O. M. Vyaselev, J. A. Martindale, V. A. Nandor, C. H. Pennington, P. C. Hammel, W. L. Hults, J. L. Smith, P. L. Kuhns, A. P. Reyes and W. G. Moulton: Phys. Rev. Lett. **82** (1999) 177.
- 51) V. F. Mitrović, H. N. Bachman, W. P. Halperin, M. Eschrig, J. A. Sauls, A. P. Reyes, P. Kuhns and W. G. Moulton: Phys. Rev. Lett. **82** (1999) 2784.
- 52) V. F. Mitrović, H. N. Bachman, W. P. Halperin, M. Eschrig and J. A. Sauls: preprint. (cond-mat/9901232)